



HAL
open science

Mass transport evolution in microfluidic thin film electrochemical reactors: New correlations from millimetric to submillimetric interelectrode distances

Faidzul Hakim Adnan, Marie-Noëlle Pons, Emmanuel Mousset

► To cite this version:

Faidzul Hakim Adnan, Marie-Noëlle Pons, Emmanuel Mousset. Mass transport evolution in microfluidic thin film electrochemical reactors: New correlations from millimetric to submillimetric interelectrode distances. *Electrochemistry Communications*, 2021, 130, pp.107097. 10.1016/j.elecom.2021.107097 . hal-03429825

HAL Id: hal-03429825

<https://hal.science/hal-03429825>

Submitted on 15 Nov 2021

HAL is a multi-disciplinary open access archive for the deposit and dissemination of scientific research documents, whether they are published or not. The documents may come from teaching and research institutions in France or abroad, or from public or private research centers.

L'archive ouverte pluridisciplinaire **HAL**, est destinée au dépôt et à la diffusion de documents scientifiques de niveau recherche, publiés ou non, émanant des établissements d'enseignement et de recherche français ou étrangers, des laboratoires publics ou privés.



Distributed under a Creative Commons Attribution - NonCommercial - NoDerivatives 4.0 International License



Short Communication

Mass transport evolution in microfluidic thin film electrochemical reactors: New correlations from millimetric to submillimetric interelectrode distances

Faidzul Hakim Adnan^a, Marie-Noëlle Pons^{a,b}, Emmanuel Mousset^{a,*}

^a Université de Lorraine, CNRS, LRGP, F-54000 Nancy, France

^b LTSER-LRGP, CNRS, Université de Lorraine, F-54000 Nancy, France



ARTICLE INFO

Keywords:

Dimensionless number
Mass transfer
Microfluidic
Micrometric
Parallel-plate reactor

ABSTRACT

Correlation of the mass transfer characteristics of microfluidic parallel-plate electrochemical reactors is proposed for the first time. Firstly, the variation in the mass transfer coefficient (k_m) ($1.61\text{--}3.94 \times 10^{-5} \text{ m s}^{-1}$) over a wide range of interelectrode distances (d_{elec}) from millimetric (3 mm) to micrometric values (100 μm) is reported. Secondly, a drastic slope change in the curve makes it possible to identify the onset of microfluidic behavior in a quantitative way for the first time, i.e. below a 1000 μm gap. Thirdly, a mathematical model is proposed which predicts k_m for any d_{elec} of interest. Fourthly, under laminar flow ($7 < \text{Reynolds } (Re) < 623$) and for temperatures in the range of 10–50 °C ($532 < \text{Schmidt } (Sc) < 3315$), new Sherwood (Sh) correlations are obtained for both microfluidic and millimetric configurations. It is thus feasible to extrapolate k_m for microfluidic electrochemical reactor scale-up.

1. Introduction

Microscale electrochemical reactors provide an interesting approach in various disciplines, such as electrosynthesis [1–5], electrodeposition [6,7], sensor development [8,9] and wastewater treatment [10–15]. Versatility, a small footprint, suitability for reactions with rapid kinetics, easy thermoregulation, independence of supporting electrolyte, mass transfer intensification and huge energy savings are among the benefits to be gained from microfluidic flow reactor technology [16–18]. Measurement of mass transfer in the submillimetric range has been studied since the early 1970s, with the development of flow rectangular channel, tubular and granular bed electrochemical reactors [19–27]. Estimating the average mass transfer coefficient (k_m) is particularly crucial in the sizing of electrochemical reactors and for scale-up studies [28]. In the case of millimetric scale reactors, the correlation of mass transfer with different geometries with or without turbulence promoters [28–33], with different electrode morphologies [34,35] as well as innovative electrolyte inlets [36,37] and agitation systems [38,39] has been widely investigated in the literature. However, more data are required on mass transfer evolution and correlation in microfluidic parallel-plate reactors at a larger scale [40]. This could be due to problems in carrying out experiments under different hydrodynamic

conditions and temperatures as well as to the difficulty of configuring 3-electrode setups with a narrow interelectrode gap [38,39]. In this paper, mass transfer evolution over a wide range of interelectrode distances (d_{elec}) from millimetric (3 mm) down to submillimetric (100 μm) values is reported for the first time, using a flow-by parallel-plate reactor with a large effective surface area. This reactor design is suitable for scaled-up industrial applications. A model has been proposed which evaluates k_m as a function of d_{elec} . Finally, a mass transfer correlation involving dimensionless numbers in microfluidic and millimetric systems is proposed.

2. Materials and methods

2.1. Electrochemical system

The electrolyte (0.5 L) was stored in a double-jacket stainless steel reservoir connected to a thermostatic bath (Bioblock Scientific, Poly-Science, Niles, IL, USA) which regulates the working temperature between 10 and 50 °C in this series of experiments. A peristaltic pump (Masterflex, Cole-Parmer, Vernon Hills, IL, USA) was used to circulate the electrolyte at the desired flow rate in batch recirculation mode. The electrochemical setup featured a parallel-plate reactor (a schematic

* Corresponding author.

E-mail address: emmanuel.mousset@univ-lorraine.fr (E. Mousset).

<https://doi.org/10.1016/j.elecom.2021.107097>

Received 22 May 2021; Received in revised form 19 July 2021; Accepted 20 July 2021

Available online 24 July 2021

1388-2481/© 2021 The Author(s). Published by Elsevier B.V. This is an open access article under the CC BY license (<http://creativecommons.org/licenses/by/4.0/>).

illustration is given in Fig. S1 in the Supplementary information). Both working and counter electrodes were planar rectangles, facing one another. 316L stainless steel (SS) (Gantois Industries, Saint-Dié-des-Vosges, France), 5 mm in thickness, was used as the working electrode. Boron-doped diamond (BDD) (DiaCCon, Fürth, Germany), 2 mm in thickness, coated on both sides with a niobium substrate 12 μm thick, served as the counter electrode. Their width (W) and length (L) were 5 and 10 cm respectively, giving an effective surface area of 50 cm^2 . Spacers made of polytetrafluoroethylene (PTFE) with different thicknesses (100, 250, 500, 1000, 1500, 2000 and 3000 μm) from Bohlender, Grünsfeld, Germany, were used to separate the working and counter electrodes. These therefore defined the values of d_{elec} investigated in this work, from the micrometric scale progressively into a typical millimetric configuration. Silver-saturated silver chloride (Ag-AgCl/Cl^-) was used as the reference electrode. This was inserted in the lower part of the cell, near the electrolyte inlet stream. The electrolyte was introduced by forced convection from the bottom of the cell, flowing upward against the gravitational force. The positioning of the reference electrode (lower part of the cell, Fig. S1) takes advantage of the gravitational force to ensure stable measurement conditions by avoiding both engorgement in the case of unstable electrolyte flow and perturbation due to gas evolution at very low applied potentials. Furthermore, the Ag-AgCl reference electrode was positioned very close to the working electrode (500 \pm 100 μm) in order to avoid ohmic loss in solution [41]. The BDD electrode features a wide potential window of water stability with the O_2 evolution reaction (OER) occurring at 2.5–2.7 V/SHE [42,43]. At this high potential OER, negligible interference from O_2 evolved on the counter electrode may be expected.

2.2. Mass transfer characterization

The mass transfer in the electrochemical cells was studied using the widely used limiting-current technique described elsewhere [41,44]. 0.5 L of electrolytic solution containing 0.05 M $\text{K}_3\text{Fe}(\text{CN})_6$, 0.10 M $\text{K}_4\text{Fe}(\text{CN})_6$ and 0.50 M Na_2CO_3 as supporting electrolyte was employed. A high concentration of supporting electrolyte was used to avoid the electro-migration effect [41,45]. Using this technique, the reduction of ferricyanide ($\text{Fe}(\text{CN})_6^{3-}$) achieved its maximum rate (limiting current plateau) so that the reduction was purely controlled by the mass transport regime. The physical properties of the electrolyte at the different temperatures under investigation [29,30,46] are given in Table S1 in the Supplementary information. Linear scan voltammetry (LSV) was carried out using a potentiostat (Ametek, Massy, France) equipped with a PMC-1000 channel that can perform both DC and AC experiments up to ± 10 V and ± 2 A, respectively. LSV was used to study the cathodic potential activity of the ferri-ferrocyanide electrolyte over a range of potentials from 0.2 to -1.6 V versus the Ag/AgCl reference electrode at a scan rate of 2.5 mV s^{-1} . Within the chosen range of flow rates, the scan rate was sufficiently slow to attain a steady state [47]. To check the influence of any dissolved O_2 in the electrolyte, preliminary experiments were conducted at both extremes (i.e. 100 and 3000 μm) as well as using a 500 μm interelectrode gap after the electrolyte had been purged of dissolved O_2 . The electrolyte in the reservoir was aerated with N_2 gas for 30 min before the LSV to eliminate dissolved O_2 . The results indicated that the limiting current plateau (just before the reduction of the solvent) was not influenced by the presence of dissolved O_2 (data not shown). The resulting limiting current values (I_{lim} in A) for different d_{elec} under the chosen operating conditions were related to the average k_m (m s^{-1}) via Eq. (1) [44]:

$$k_m = \frac{I_{\text{lim}}}{nFSC_{\text{sol}}} \quad (1)$$

where n is the number of electrons involved in the reduction reaction of ferri- to ferrocyanide (i.e. 1), F is Faraday's constant (96485 C mol^{-1}), S is the effective surface area of the working electrode (m^2) and C_{sol} is the

molar concentration of ferricyanide in the bulk solution (mol m^{-3}).

The flow rate varied from 10 to 600 mL min^{-1} , when d_{elec} was increased from 100 to 3000 μm . Across all investigated values of d_{elec} and for relevant comparison, the electrolyte flow was kept within the laminar regime with Reynolds (Re) values in the range 7 to 623. Owing to the entrance manifolds of the tube-type entry of the electrochemical cell, under similar hydrodynamic regimes, the electrolyte recirculating zone in the reactor was considered minimal in all investigated configurations [36,48,49].

3. Results and discussion

3.1. Mass transfer behavior over a wide range of interelectrode distances

Average k_m values over the wide range of d_{elec} , obtained from the plateau of I_{lim} identified on voltammograms for the different values of d_{elec} (Fig. S2), are shown in Fig. 1. Interestingly, two distinct behaviors of k_m were observed as a first approach. The increase in k_m in the millimetric range from 3000 μm down to 1000 μm seemed linear (slope: -10^{-3} s^{-1} , coefficient of determination $R^2 = 0.91$). For values lower than 1000 μm , k_m increased drastically as d_{elec} decreased into the micrometric range. This trend suggests that the mass transfer was massively enhanced while transitioning from a millimetric to a micrometric gap, which supports the interest in microfluidic reactors for transfer intensification [14,16,50–55]. The range of values of k_m determined under both millimetric and micrometric configurations in this work are in close agreement with those reported in the literature (Table S2 in the Supplementary information). In the millimetric range, k_m values of $1.61 \times 10^{-5} \text{ m s}^{-1}$ and $1.82 \times 10^{-5} \text{ m s}^{-1}$ were obtained for 3000 μm and 1000 μm , respectively, compared with reported values of k_m between 0.30 and $1.20 \times 10^{-5} \text{ m s}^{-1}$ for 5000 μm [56] and $1.60 \times 10^{-5} \text{ m s}^{-1}$ for 1000 μm [28].

The Levich equation (Eq. (2)) has been widely used in the literature to relate I_{lim} to electrolyte volume flow rate in thin rectangular channel electrode reactors [19,57,58].

$$I_{\text{lim}} = 0.925nFWC_{\text{sol}}(D_L X_c)^{2/3} \left(\frac{\dot{V}_F}{h^2 d} \right)^{1/3} \quad (2)$$

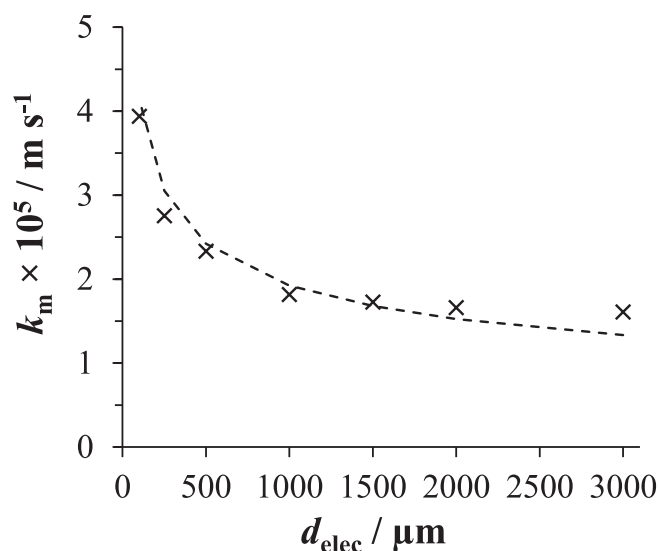


Fig. 1. Variation of experimental and theoretical average values of k_m as a function of d_{elec} . Operating conditions: Flow rate: 10–600 mL min^{-1} , temperature: 25 $^\circ\text{C}$, identical cross-sectional electrolyte velocity (u_1): 4 m min^{-1} and electrolyte residence time (τ): 0.025 min (see Text S1 in the Supplementary Information).

where

$$\dot{V}_F = u_L W d_{\text{elec}} \quad (3)$$

$$h = \frac{d_{\text{elec}}}{2} \quad (4)$$

Here W is the electrode width (in m), D_L is the diffusion coefficient (in $\text{m}^2 \text{s}^{-1}$), x_c is the electrode length (equivalent to L , in m), \dot{V}_F is the volumetric flow rate (in $\text{m}^3 \text{s}^{-1}$), h is half the cell depth (in m), d is the channel width (equivalent to W in this work, in m) and u_L is the cross-sectional velocity (in m s^{-1} , defined as Eq. S1 in the [Supplementary Information](#)). Equation (2) is ideally applicable under conditions where $h \ll d$, there is a sufficiently large electrode area, the electrolyte flow rate is not too low and the profile of electrolyte flow velocity in the channel is parabolic [19]. Relating Eq. (1) and Eq. (2) yields an expression of average k_m as a function of d_{elec} (Eq. (5)):

$$k_m = \frac{2.94 D_L^{2/3} u_L^{1/3} W L^{2/3}}{S d_{\text{elec}}^{1/3}} \quad (5)$$

A slight adjustment of the coefficient in Eq. (2) was made to match the experimental data. This deviation could be due to the fact that direct application of Eq. (2) is not ideal under conditions where the electrode width and channel width are identical ($W = d$), in which an edge effect could not be neglected [19,40]. The plot of experimental and theoretical k_m versus d_{elec} is given in Fig. 1. The theoretical curve matches its experimental counterpart well, with a deviation of 0.000187 when subject to root mean square error (RMSE) evaluation (Eq. (6)) [59]:

$$\text{RMSE} = \sqrt{\frac{\sum_{i=1}^K (y_i - y_i')^2}{K}} \quad (6)$$

where y_i' is the experimental value, y_i is the theoretical value and K is the number of measurements.

3.2. Mass transfer correlations in microfluidic and millimetric parallel-plate electrochemical reactors

Mass transfer correlations were evaluated using electrochemical reactors equipped with d_{elec} of 100 and 500 μm (representing micrometric setups) and 3000 μm (representing a millimetric setup). The variation of mass transfer with fluid hydrodynamics, fluid physicochemical properties and electrochemical reactor geometry can be expressed using the theoretical dimensionless Sherwood (Sh) correlation incorporating Re , Schmidt (Sc), and dimensionless distance (Le) numbers as well as the d_{elec}/W aspect ratio as given in Eq. (7) [60]:

$$Sh = a Re^b Sc^c Le^d \left(\frac{2}{1 + \frac{d_{\text{elec}}}{W}} \right)^{1/3} \quad (7)$$

The form of expression in Eq. (7) is valid with strict respect to the L ev eque approximation [57,61] which assumes that: (i) the electrolyte is incompressible, having constant physical properties; (ii) the flow is in laminar steady-state, becoming fully developed after a certain entry length for a given reactor geometry; (iii) mass transport is due to convection and diffusion; (iv) electrolyte flow is treated as bidimensional in the x-y planes (Fig. S1); (v) molecular diffusion of reactive species only occurs along the x-axis (normal to the electrodes); (vi) friction at walls induces retardation and produces a parabolic velocity profile with maximum velocity at the center of the channel; and (vii) the diffusional double-layer is a lot smaller than the hydrodynamic boundary layer. This dimensionless expression is particularly useful in estimating the average k_m values during scaling-up or scaling-down of an electrochemical reactor under the operating conditions of interest. The entry length (E_L) was evaluated via Eq. (8) [61,62] and this increased from

0.027 to 21.7 mm when d_{elec} was increased from 100 to 3000 μm (Fig. S3). Re , Sc and Le are defined by Eqs. (9)–(11) whilst a , b , c and d are constant parameters.

$$E_L = 0.01 d_H Re \quad (8)$$

$$Re = \frac{u_L d_H}{\nu_L} \quad (9)$$

$$Sc = \frac{\nu_L}{D_L} \quad (10)$$

$$Le = \frac{d_H}{L} \quad (11)$$

$$d_H = \frac{2W d_{\text{elec}}}{W + d_{\text{elec}}} \quad (12)$$

ν_L is the kinematic viscosity in $\text{m}^2 \text{s}^{-1}$ at the operating temperature [29,30,46] (Table S1). d_H is the hydraulic diameter in m.

To establish the theoretical Sh correlation, k_m values were measured at different electrolytic flow rates and temperatures. Experimental Sh values were computed using Eq. (13) [44] and plotted against various investigated Re and Sc numbers. The coefficients a , b , c and d were extracted from the best fit between theoretical and experimental Sh plots.

$$Sh = \frac{k_m d_H}{D_L} \quad (13)$$

The influence of electrolyte flow rate and temperature on k_m for each selected configuration is presented in Fig. 2. k_m increased with increasing flow rate across both configurations at constant temperature (Fig. 2(a)). This finding is expected owing to the enhancement of mass transport for the $\text{Fe}(\text{CN})_6^{3-}$ reduction reaction when higher flow rates were tested. It can be observed that the increase in k_m with increasing electrolyte flow rate was much more pronounced in the microfluidic devices (100 and 500 μm) compared to the setup with a distance of 3000 μm (Fig. 2(a)). The highest value of k_m ($5.06 \times 10^{-5} \text{ m s}^{-1}$ at 0.05 L min^{-1}) was achieved when the electrochemical reactor was equipped with a 100 μm interelectrode gap. In addition, when the temperature was increased from 10 to 50 $^\circ\text{C}$, k_m increased from 3.28×10^{-5} to $5.22 \times 10^{-5} \text{ m s}^{-1}$ for the 100 μm gap, from 1.66×10^{-5} to $3.11 \times 10^{-5} \text{ m s}^{-1}$ for the 500 μm gap and from 1.20×10^{-5} to $2.41 \times 10^{-5} \text{ m s}^{-1}$ for the 3000 μm gap (Fig. 2(b)). These trends are due to the increase in diffusivity of $\text{Fe}(\text{CN})_6^{3-}$ -reducing species with temperature [46,63,64].

Using the k_m values obtained under different operating conditions, experimental values of Sh were obtained as illustrated in Fig. 3. The best fitting of Eq. (7) to the experimental data of each submillimetric and millimetric configuration was achieved when the coefficients a , b , c and d took the values provided in Table 1. The value of coefficient a varied slightly: it decreased from 3.00 to 2.31 from 100 μm to 500 μm d_{elec} but increased again to 3.01 when using the 3000 μm configuration. The values are within the range reported in the literature [60,65]. The variation of b between 0.32 and 0.37 corroborated the Re exponent value of close to 0.30 reported in the literature, which corresponds to fully developed laminar flow [34,37,60,65,66]. The widely reported 1/3 ratio of the Sc exponent c and the Le exponent d were obtained to match the experimental data under all three setups [30,32,34,37,60,65,66].

The fitting of the theoretical Sh correlations with the experimental data for all three d_{elec} configurations were evaluated using RMSE (Eq. (6)). Deviations of 0.038, 0.056 and 0.024 were calculated between logarithmic plots of the theoretical-experimental Sh values against Re for 100, 500 and 3000 μm configurations, respectively. For Sc , the theoretical plot deviated from the experimental data by 0.070, 0.047 and 0.026 for gaps of 100, 500 and 3000 μm , respectively. Therefore, the theoretical Sh correlations fitted very well with their experimental counterparts.

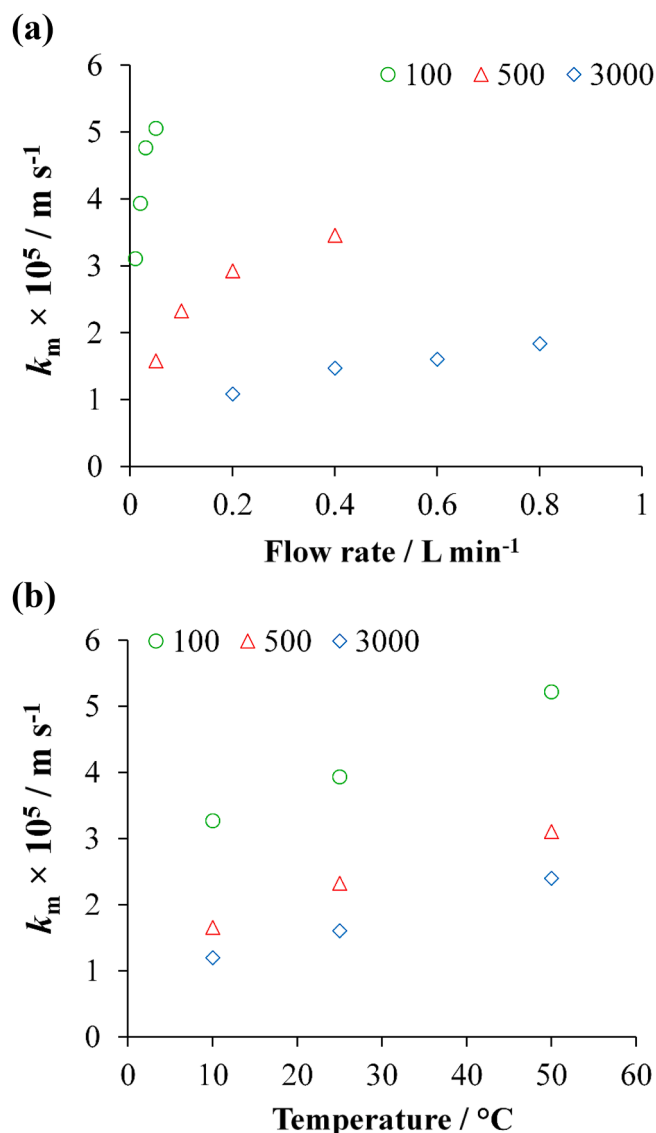


Fig. 2. k_m as a function of (a) electrolyte flow rate and (b) temperature for d_{elec} values of 100, 500 and 3000 μm . Operating conditions: (a) temperature = 25 $^\circ\text{C}$ and (b) flow rates = 0.02, 0.10 and 0.60 L min^{-1} for d_{elec} values of 100, 500 and 3000 μm , respectively.

Given the trends in the a , b , c and d coefficients under the wide range of d_{elec} values studied, under a fully developed laminar regime, an average Sh correlation can be proposed (see Eq. (14)):

$$Sh_{\text{ave}} = 2.7733Re^{0.35}Sc^{1/3}Le^{1/3} \left(\frac{2}{1 + \frac{d_{\text{elec}}}{W}} \right)^{1/3} \quad (14)$$

The average Sh correlation is in close agreement with that proposed by Pickett et al. [60], with the a coefficient slightly higher in the current work. This could be attributed to the larger surface area used here (50 cm^2 vs. 16 cm^2 in [60]) as well as enhancement of mass transport in the microfluidic reactor.

4. Conclusions

The variation in k_m as a function of d_{elec} from the millimetric to the micrometric range is reported for the first time. A novel single equation which estimates k_m over a wide range of d_{elec} values has been proposed. It highlights the inverse relationship between k_m and d_{elec} , where k_m

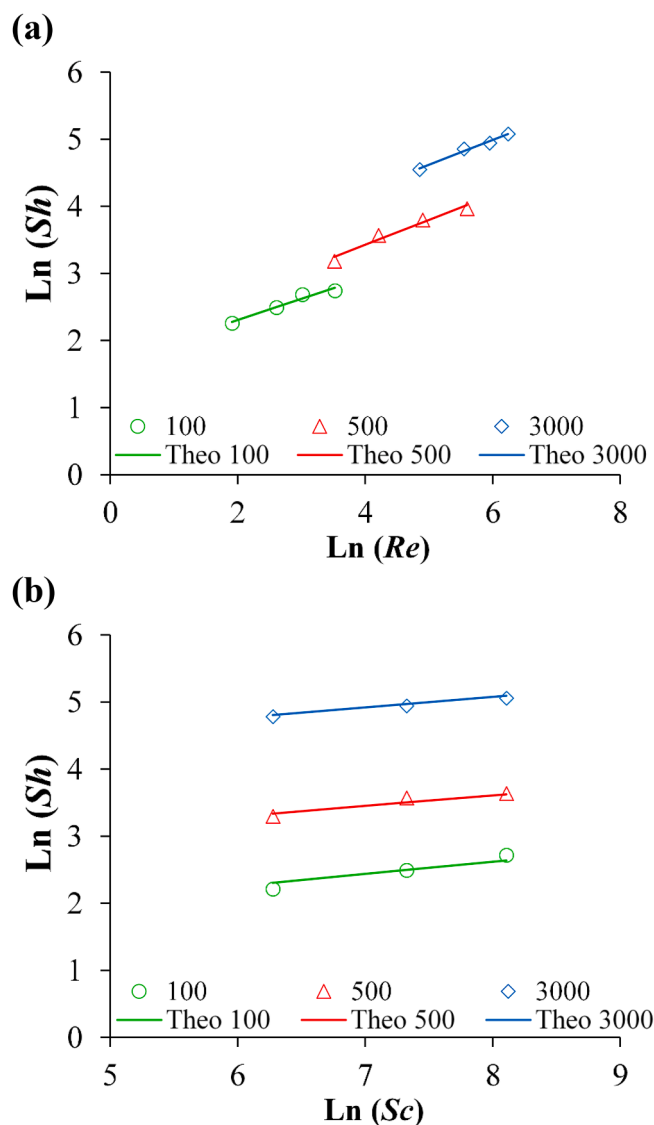


Fig. 3. Experimental (symbol) versus theoretical Sh correlations (continuous line) as a function of (a) Re and (b) Sc numbers. Operating conditions: (a) temperature = 25 $^\circ\text{C}$ and (b) flow rates = 0.02, 0.10 and 0.60 L min^{-1} for d_{elec} values of 100, 500 and 3000 μm , respectively.

Table 1

Fitted values of a , b , c and d parameters in the theoretical Sh correlation in parallel-plate electrochemical reactors with microfluidic and millimetric configurations under a laminar regime.

Configuration	a	b	c	d	Re ranges	Sc ranges
Thin film reactor (distance: 100 μm)	3.00	0.32	0.33	0.33	7–34	532–3315
Thin film reactor (distance: 500 μm)	2.31	0.37	0.33	0.33	34–269	532–3315
Parallel-plate (distance: 3000 μm)	3.01	0.37	0.33	0.33	128–623	532–3315

values increase greatly at distances below 1000 μm . Using experimental k_m data in submillimetric as well as millimetric configurations at varying flow rates ($7 < Re < 623$) and temperatures ($532 < Sc < 3315$), mass transport correlations have been established that take into consideration not only fluid properties but also electrochemical reactor hydrodynamics and geometry. The theoretical Sh number plots match very well

with their corresponding experimental values. The newly established Sh correlation in this work covers a wide range of interelectrode distances. The results were obtained using an electrochemical cell whose design is well adapted for multidisciplinary applications on a larger scale, whilst the robustness of the Sh correlation was justified experimentally. The results presented herein will be particularly helpful for k_m estimation in parallel-plate reactors under wide range of d_{elec} values (i.e. from several tens of micrometers to several millimeters) under given operating conditions. These expressions should be particularly suitable for micro-distances that can be useful for significant mass transfer intensification, unlike the millimetric or even centimetric distances often implemented.

CRedit authorship contribution statement

Faidzul Hakim Adnan: Methodology, Investigation, Formal analysis, Writing - original draft. **Marie-Noëlle Pons:** Supervision, Writing - review & editing, Funding acquisition. **Emmanuel Mousset:** Conceptualization, Methodology, Validation, Supervision, Writing - review & editing, Project administration, Resources, Funding acquisition.

Declaration of Competing Interest

The authors declare that they have no known competing financial interests or personal relationships that could have appeared to influence the work reported in this paper.

Acknowledgments

The authors would like to thank the French Ministry of Higher Education and Research (MESRI) for financial support of the doctorate program of Faidzul Hakim Adnan as well as other funding from Carnot ICEEL, LTSER Zone Atelier du Bassin de la Moselle (ZAM) and the European regional development fund program (CPER SusChemProc).

Appendix A. Supplementary data

Supplementary data to this article can be found online at <https://doi.org/10.1016/j.elecom.2021.107097>.

References

- [1] C.A. Paddon, M. Atobe, T. Fuchigami, P. He, P. Watts, S.J. Haswell, G.J. Pritchard, S.D. Bull, F. Marken, *J. Appl. Electrochem.* 36 (2006) 617.
- [2] A.A. Fogueiras-Amador, K. Philipps, S. Guilbaud, J. Poelakker, T. Wirth, *Angew. Chem. Int. Ed.* 56 (2017) 15446–15450.
- [3] C. Renault, J. Roche, M.R. Ciumag, T. Tzedakis, S. Colin, K. Serrano, O. Reynes, C. André-Barrès, P. Winterton, *J. Appl. Electrochem.* 42 (2012) 667–677.
- [4] M. Atobe, H. Tateno, Y. Matsumura, *Chem. Rev.* 118 (2018) 4541–4572.
- [5] A. Ziogas, G. Kolb, M. O'Connell, A. Attour, F. Lapique, M. Matlosz, S. Rode, *J. Appl. Electrochem.* 39 (2009) 2297.
- [6] C. Léger, J. Elezgaray, F. Argoul, *J. Electroanal. Chem.* 486 (2000) 204–219.
- [7] M. Rosso, E. Chassaing, J.N. Chazalviel, T. Gobron, *Electrochim. Acta* 47 (2002) 1267–1273.
- [8] S. Park, J.H. Park, S. Hwang, J. Kwak, *Electrochem. Commun.* 68 (2016) 76–80.
- [9] H. Lee, T.K. Choi, Y.B. Lee, H.R. Cho, R. Ghaffari, L. Wang, H.J. Choi, T.D. Chung, N. Lu, T. Hyeon, S.H. Choi, D.-H. Kim, *Nat. Nanotechnol.* 11 (2016) 566–572.
- [10] S. Zhang, M. Sun, T. Hedtke, A. Deshmukh, X. Zhou, S. Weon, M. Elimelech, J.-H. Kim, *Environ. Sci. Technol.* 54 (2020) 10868–10875.
- [11] M. Rodríguez, M. Muñoz-Morales, J.F. Perez, C. Saez, P. Cañizares, C.E. Barrera-Díaz, M.A. Rodrigo, *Ind. Eng. Chem. Res.* 57 (2018) 10709–10717.
- [12] O. Scialdone, A. Galia, S. Sabatino, *Appl. Catal. B* 148–149 (2014) 473–483.
- [13] S. Sabatino, A. Galia, O. Scialdone, *ChemElectroChem* 3 (2016) 83–90.
- [14] E. Mousset, *Electrochem. Commun.* 118 (2020), 106787.
- [15] M.L. Satuf, J. Macagno, A. Manassero, G. Bernal, P.A. Kler, C.L.A. Berli, *Appl. Catal. B* 241 (2019) 8–17.
- [16] H.S. White, K. McKelvey, *Curr. Opin. Electrochem.* 7 (2018) 48–53.
- [17] W.B. Zimmerman, *Chem. Eng. Sci.* 66 (2011) 1412–1425.
- [18] K. Jähnisch, V. Hessel, H. Löwe, M. Baerns, *Angew. Chem. Int. Ed.* 43 (2004) 406–446.
- [19] R.G. Compton, P.R. Unwin, *J. Electroanal. Chem. Interfacial Electrochem.* 205 (1986) 1–20.
- [20] J.A. Cooper, R.G. Compton, *Electroanalysis* 10 (1998) 141–155.
- [21] M.D. Birkett, A. Kuhn, *Electrochim. Acta* 22 (1977) 1427–1429.
- [22] I. Roušar, J. Hostomský, V. Cezner, B. Štverák, *J. Electrochem. Soc.* 118 (1971) 881.
- [23] K. Aoki, K. Tokuda, H. Matsuda, *J. Electroanal. Chem. Interfacial Electrochem.* 209 (1986) 247–258.
- [24] K. Yunus, A.C. Fisher, *Electroanalysis* 15 (2003) 1782–1786.
- [25] P.R. Unwin, R.G. Compton, Chapter 6: The use of channel electrodes in the investigation of interfacial reaction mechanisms, in: R.G. Compton (Ed.), *Comprehensive Chemical Kinetics*, Elsevier, 1989, pp. 173–296.
- [26] D.J. Pickett, Design of plug flow electrochemical reactors, in: *Electrochemical Reactor Design*, Elsevier Science Publishing Company, 1979, pp. 171–280.
- [27] D.R. Gabe, D.J. Robinson, *Electrochim. Acta* 17 (1972) 1121–1127.
- [28] Á. Anglada, A.M. Urriaga, I. Ortiz, *J. Hazard. Mater.* 181 (2010) 729–735.
- [29] A.A. Wrang, A.A. Leontaritis, *Chem. Eng. J.* 66 (1997) 1–10.
- [30] M. Griffiths, C.P. de León, F.C. Walsh, *Am. Inst. Chem. Eng.* 51 (2005) 682–687.
- [31] C.A. Martínez-Huitle, S. Ferro, A. De Battisti, *J. Appl. Electrochem.* 35 (2005) 1087–1093.
- [32] T.R. Ralph, M.L. Hitchman, J.P. Millington, F.C. Walsh, *Electrochim. Acta* 41 (1996) 591–603.
- [33] F.C. Walsh, C. Ponce de León, *Electrochim. Acta* 280 (2018) 121–148.
- [34] N. Tzanetakis, K. Scott, W.M. Taama, R.J.J. Jachuck, *Appl. Therm. Eng.* 24 (2004) 1865–1875.
- [35] M. Cruz-Díaz, F.F. Rivera, E.P. Rivero, I. González, *Electrochim. Acta* 63 (2012) 47–54.
- [36] A. Djati, M. Brahimi, J. Legrand, B. Saidani, *J. Appl. Electrochem.* 31 (2001) 833–837.
- [37] D.J. Pickett, K.L. Ong, *Electrochim. Acta* 19 (1974) 875–882.
- [38] S. Coleman, S. Roy, *Chem. Eng. Sci.* 113 (2014) 35–44.
- [39] S.J. Coleman, S. Roy, *Ultrason. Sonochem.* 42 (2018) 445–451.
- [40] D. Pauwels, B. Geboes, J. Hereijgers, D. Choukroun, K. De Wael, T. Breugelmans, *Chem. Eng. Res. Des.* 128 (2017) 205–213.
- [41] J.R. Selman, C.W. Tobias, Mass-transfer measurements by the limiting-current technique, in: T.B. Drew, G.R. Cokelet, J.W. Hoopes, T. Vermeulen (Eds.), *Advances in Chemical Engineering*, Academic Press, 1978, pp. 211–318.
- [42] P.A. Michaud, M. Panizza, L. Ouattara, T. Diaco, G. Foti, C. Cominellis, *J. Appl. Electrochem.* 33 (2003) 151–154.
- [43] A. Kraft, *Int. J. Electrochem. Sci.* 2 (2007) 355–385.
- [44] P. Cañizares, J. García-Gómez, I. Fernández de Marcos, M.A. Rodrigo, J. Lobato, *J. Chem. Educ.* 83 (2006) 1204.
- [45] F.H. Adnan, E. Mousset, S. Pontvianne, M.-N. Pons, *Electrochim. Acta* 387 (2021), 138487.
- [46] H. Saraç, M.A. Patrick, A.A. Wrang, *J. Appl. Electrochem.* 23 (1993) 51–55.
- [47] A.C. Fisher, R.G. Compton, *J. Appl. Electrochem.* 22 (1992) 38–42.
- [48] A.A. Wrang, D.J. Tagg, M.A. Patrick, *J. Appl. Electrochem.* 10 (1980) 43–47.
- [49] J.E. Terrazas-Rodríguez, S. Gutiérrez-Granados, M.A. Alatorre-Ordaz, C. Ponce de León, F.C. Walsh, *Electrochim. Acta* 56 (2011) 9357–9363.
- [50] G. Gao, Q. Zhang, Z. Hao, C.D. Vecitis, *Environ. Sci. Technol.* 49 (2015) 2375–2383.
- [51] S. Franssen, J. Franssaer, S. Kuhn, *Electrochim. Acta* 292 (2018) 914–934.
- [52] P. Ma, H. Ma, S. Sabatino, A. Galia, O. Scialdone, *Chem. Eng. J.* 336 (2018) 133–140.
- [53] J.F. Pérez, J. Llanos, C. Sáez, C. López, P. Cañizares, M.A. Rodrigo, *Chem. Eng. J.* 351 (2018) 766–772.
- [54] J.F. Pérez, J. Llanos, C. Sáez, C. López, P. Cañizares, M.A. Rodrigo, *Sup. Purif. Technol.* 208 (2019) 123–129.
- [55] E. Mousset, M. Puce, M.N. Pons, *ChemElectroChem* 6 (2019) 2908–2916.
- [56] A.M. Polcaro, A. Vacca, M. Mascia, S. Palmas, J. Rodriguez Ruiz, *J. Appl. Electrochem.* 39 (2009) 2083.
- [57] J.C. Eklund, A.M. Bond, J.A. Alden, R.G. Compton, Perspectives in modern voltammetry: basic concepts and mechanistic analysis, in: D. Bethell (Ed.), *Advances in Physical Organic Chemistry*, Academic Press, 1999, pp. 1–120.
- [58] C.A. Paddon, G.J. Pritchard, T. Thiemann, F. Marken, *Electrochem. Commun.* 4 (2002) 825–831.
- [59] E. Mousset, L. Quackenbush, C. Schondek, A. Gerardin-Vergne, S. Pontvianne, S. Kmietek, M.-N. Pons, *Electrochim. Acta* 334 (2020), 135608.
- [60] D.J. Pickett, B.R. Stanmore, *J. Appl. Electrochem.* 2 (1972) 151–156.
- [61] F. Cœuret, A. Storck, *Revue des corrélations, in: Éléments de Génie Électrochimique*, Lavoisier, Paris, 1993, pp. 129–165.
- [62] L.S. Han, *J. Appl. Mech.* 27 (1960) 403–409.
- [63] E. Eroğlu, S. Yapıcı, O.N. Şara, *J. Chem. Eng. Data* 56 (2011) 3312–3317.
- [64] A.J. Arvía, S.L. Marchiano, J.J. Podestá, *Electrochim. Acta* 12 (1967) 259–266.
- [65] T.P. Szanto, I. White, F.C. Walsh, in: *4th European Symposium on Electrochemical Engineering*, Prague, Czech Republic, 1996, pp. 273.
- [66] J.L.C. Santos, V. Gerales, S. Velizarov, J.G. Crespo, *Chem. Eng. J.* 157 (2010) 379–392.